MOLECULAR AND CELLULAR BIOLOGY, Apr. 2010, p. 1937–1945 Vol. 30, No. 8
0270-7306/10/$12.00 doi:10.1128/MCB.01370-09

Uncoupling of Expression of an Intronic MicroRNA and Its Myosin Host Gene by Exon Skipping▽

Matthew L. Bell, Massimo Buvoli, and Leslie A. Leinwand*

Department of Molecular, Cellular, and Developmental Biology, University of Colorado, Boulder, Colorado 80309

Received 14 October 2009/Returned for modification 14 November 2009/Accepted 28 January 2010

The ancient MYH7b gene, expressed in striated muscle and brain, encodes a sarcomeric myosin and the intronic microRNA miR-499. We find that skipping of an exon introduces a premature termination codon in the transcript that downregulates MYH7b protein production without affecting microRNA expression. Among other genes, endogenous miR-499 targets the 3′ untranslated region of the transcription factor Sox6, which in turn acts as a repressor of MYH7b transcriptional activity. Thus, concerted transcription and alternative splicing uncouple the level of expression of MYH7b and miR-499 when their coexpression is not required.

Skeletal and cardiac muscle exhibit a broad range of contractile characteristics and adaptive responses that are controlled, at least in part, by sarcomeric myosins, a multigene family of actin-based motors that convert chemical energy released from ATP hydrolysis into mechanical force. In addition to the eight well-characterized myosin heavy chain (MYH) isoforms expressed in heart and skeletal muscle, three more ancient myosin genes, MYH7b (MYH14), MYH15, and MYH16, have been identified (13). In humans, the MYH16 gene is a pseudogene by virtue of a frameshift mutation and consequent premature termination codon (PTC). Remarkably, the gene is not mutated in other nonhuman primates and appears to regulate the fiber size of the masticatory muscles (35). Phylogenetic analysis suggests that MYH7b is most closely related to α- and β-cardiac myosins, with 69% amino acid identity. Moreover, these three related myosin genes encode microRNAs (miRNAs) in one of their introns (MYH-α, miR-208a; MYH-β, miR-208b; and MYH7b, miR-499) (40, 41). In particular, miR-208a has been shown to be a key mediator of the stress response and a regulator of hypertrophy and electrical conduction in the mouse heart (6, 41). Since MYH7b mRNA levels appear much lower than those of other muscle myosins, the role of MYH7b protein in vertebrate muscle remains unclear.

Here, we show that MYH7b expression is controlled transcriptionally by different stimuli, as well as posttranscriptionally, through a unique alternative splicing event. Moreover, we show that miR-499 acts in a regulatory feedback circuit to control MYH7b activity. Our data reveal the complexity of MYH7b gene regulation and unveil a novel mechanism that uncouples host gene-microRNA coexpression.

MATERIALS AND METHODS

Animal use and care. C57/BL6 mice used in the experiments were allowed access to standard soy-based rodent chow and water *ad libitum*. Unless otherwise noted, C57/BL6 male mice 12 weeks of age were used in the experiments. For altered thyroid hormone conditions, mice were fed an iodine-deficient chow supplemented with 0.15% propylthiouracil ([PTU] Harlan Teklad diet composition TD.95125) *ad libitum* for 30 days. Mice treated with PTU and triiodothyronine (T_3) were injected intraperitoneally with 0.2 μg/g T_3 on days 29 and 30 of PTU diet ingestion. Four mice from each thyroid condition were sacrificed at 12 weeks of age, and tissues were rapidly excised and frozen. All research involving the use of mice was performed in strict accordance to protocols approved by the Institutional Animal Use and Care Committee at the University of Colorado. Female, 1- to 1.5-year old zebrafish were provided by the lab of Angeles Ribera, University of Colorado Health Science Center.

Cell culture. C2C12 myoblasts were maintained in growth medium (Dulbeco's modified Eagle medium supplemented with 20% fetal bovine serum, 2% L-glutamine, and 1% penicillin-streptomycin antibiotics). To induce differentiation into myotubes, confluent C2C12 myoblasts were subjected to serum removal (Dulbeco's modified Eagle medium supplemented with 2% calf serum, 2% L-glutamine, and 1% penicillin/streptomycin antibiotics) for the number of days specified in the figure legends. For transfection experiments, myoblasts were treated as described below while approximately 70% confluent. Cells were then allowed to recover overnight in growth medium before serum removal to induce differentiation. COS-7 cells were maintained as specified by the ATCC. For prevention of nonsense-mediated decay via inhibition of protein synthesis, C2C12 cells were allowed to differentiate for 2 days, after which the cells were treated with cycloheximide for 2 h at a concentration of 100 μg/ml, as previously described (7).

RNA extraction and RT-PCR. Total RNA was isolated from cultured cells, zebrafish tissue, and mouse tissues using Tri Reagent (Molecular Research Center, Inc.) according to the manufacturer's instructions. Human brain, skeletal muscle, and heart total RNA were obtained from Stratagene (MVP Total RNA). Random hexamer-primed cDNA for reverse transcription-PCR (RT-PCR) analysis was synthesized with Superscript III reverse transcriptase (Invitrogen) according to the manufacturer's instructions.

Real-time PCR analysis. Real-time PCR was performed on an Applied Biosystems 7500 Fast Real-Time PCR system using SYBR Green PCR Mastermix (Applied Biosystems) in combination with standard oligonucleotide primers or TaqMan Universal PCR Master Mix (Applied Biosystems) in combination with TaqMan primer pairs and probe. Changes in miR-499 expression were assessed in reference to snoRNA202 using TaqMan microRNA assays (Applied Biosystems), according to the manufacturer's directions, and analyzed using the comparative threshold cycle (C_T) method.

miRNA Northern blotting protocol. Northern blot analysis for miRNA expression was performed on 20 μg of total RNA from each sample. Samples were separated on a 15% acrylamide urea denaturing gel and transferred by electrophoresis to Nytran SPC nylon membrane (Whatman). RNA was then UV cross-linked according to the manufacturer's instructions. Blots were hybridized overnight at 42°C in 0.2 M Na_2HPO_4–7% SDS with oligonucleotide probes labeled with [γ-^{32}P]ATP. Following hybridization, blots were washed twice for 15 min at 42°C in 2× SSPE (1× SSPE is 0.18 M NaCl, 10mM NaH_2PO_4, and 1 mM EDTA [ph 7.7])–0.1% SDS. Band intensities were quantified by phosphorimager analysis (Storm 860 image analyzer; Molecular Dynamics) and analyzed with ImageQuant TL software (Amersham Biosciences).

* Corresponding author. Mailing address: Department of Molecular, Cellular, and Developmental Biology, University of Colorado, UCB 347, Boulder CO, 80309. Phone: (303) 492-7606. Fax: (303) 492-8907. E-mail: Leslie.Leinwand@Colorado.edu.

▽ Published ahead of print on 2 February 2010.

DNA constructs. MYH-β and MYH7b mouse promoter sequences (1 kb each) were amplified from genomic DNA by PCR and cloned into the pGL3-Basic plasmid upstream of the firefly luciferase gene. The proximal 1-kb portion of the mouse Sox6 3′ untranslated region ([UTR] pGL-Sox6) containing four predicted miR-499 binding sites was amplified from mouse heart total RNA by RT-PCR and cloned into pGL3-Control (Promega) downstream of the firefly luciferase gene. Similarly, 3′ UTRs from mouse Thrap1, Mapk6, myostatin, and Sp3 were also cloned into pGL3-Control downstream of the firefly luciferase gene. The Sox6 expression construct (pcSox6) was made by amplifying the Sox6 coding region from mouse heart cDNA and inserting it into pcDNA3 (Invitrogen). The miR-499 expression construct was made by fusing the genomic sequence of mouse MYH7b exons 19 and 20 to the beta-globin 5′ and 3′ UTR and cloning into pcDNA3. All oligonucleotide sequences and cloning strategies are available upon request.

Exon 7 alternative splicing PCR analysis. Quantifications of the alternative splicing products were carried out by PCR using Cy5-labeled primers located in MYH7b exons 5 and 9, MYH7b exon 5 and exon 7/8 junction, or MYH-β exons 6 and 9, as previously described (33). Reaction products amplified for 25 to 35 cycles were separated on a nondenaturing 8% polyacrylamide gel, and fluorescent products were quantified by phosphorimager (Storm 860 image analyzer; Molecular Dynamics) and analyzed with ImageQuant TL software (Amersham Biosciences). Zebrafish analysis was performed using standard PCRs.

Identification of *cis*-regulatory regions of MYH7b. Conserved *cis*-regulatory elements in the MYH7b gene were identified using a pattern-defined regulatory island (PRI) algorithm (8). The PRI algorithm identifies clusters of predicted transcription factor binding sites that are conserved in order and spacing across the human, rat, and mouse genomes.

Reporter assays. For promoter activity, 0.5 μg of each promoter construct and 0.5 μg of the internal control reporter plasmid pRL-TK (Promega) were cotransfected into C2C12 myoblasts with Lipofectamine 2000 (Invitrogen) according to the manufacturer's instructions. For the effect of Sox6 overexpression on promoter activity, 0.5 μg of an MYH7b 1-kb promoter construct, 0.3 μg of empty expression vector or pcSox6, and 0.2 μg of pRL-TK were cotransfected into C2C12 myoblasts. For miR-499 targeting assays, COS cells were transfected with 0.4 μg of pGL3 3′ UTR construct, 0.4 μg of the empty expression vector or miR-499 expression vector, and 0.2 μg of pRL-TK. Cells were collected at 24 h posttransfection, and luciferase assays were performed with a dual-luciferase reporter system (Promega) according to the manufacturer's instructions. All experiments were performed in quadruplicate.

MYH7b protein purification and MS. Sarcomeric proteins were isolated from mouse soleus in myosin extraction buffer as previously described (1), followed by further enrichment for myosin proteins by two rounds of low-salt precipitation (10 mM TES [*N*-tris(hydroxymethyl)methyl-2-aminoethanesulfonic acid], 150 mM NaCl, 3.5 mM EDTA, pH 7.3), centrifugation for 1 h (20,000 × *g* at 4°C), and resuspension in high-salt buffer (10 mM TES, 300 mM NaCl, 3.5 mM EDTA, pH 7.3). Protein samples were submitted for liquid chromatography-tandem mass spectrometry (LC-MS/MS) to the University of Colorado Cancer Center Proteomics Core.

NRVM preparation and infection. Neonatal rat ventricular myocytes (NRVMs) were isolated and cultured from neonatal Sprague-Dawley rats as previously described (25). Adenoviral infection was performed at a multiplicity of infection (MOI) of 100. For phenylephrine (PE) experiments, 20 μM PE or an equivalent volume of dimethyl sulfoxide (DMSO) vehicle was added to the NRVM plates at 24 h after isolation when the growth medium was changed to serum-free medium. Plates were collected after 48 h of treatment for RNA isolation and analysis.

Oligonucleotide probes and primers. For mouse real-time quantitative PCR, the following primers were used: for MYH-β (forward [F], 5′-TTC CTT ACT TGC TAC CCT C-3′; reverse [R], 5′-CTT CTC AGA CTT CCG CAG-3′), MYH7b (F, 5′-CTC AAG CGG GAG AAC AAG AAT C-3; R, 5′-CTG AGG CTG ACC TGG TCT GTA A-3′), MYH-IIb (F, 5′-CAG GTC AAC AAG CTG CGG GTG-3′; R, 5′-GAT ATA CAG GAC AGT GAC AAA GAA CG-3′), and 18S (F, 5′-GCC GCT AGA GGT GAA ATT CTT G-3′; R, 5′-CTT TCG CTC TGG TCC GTC TT-3′). For exon 7 alternative splicing, the following were used: mouse MYH7b (Cy5 Exon 5 F, 5′-Cy5-CAA GGG CAA GCG TCG CTC C-3′; Exon 7/8 R, 5′-AAA TTG TGC CTT CTT GCC CG-3′; Exon 9 R, 5′-CTC CAT GGC AGG GTT AGC CTC-3′), human MYH7b (Cy5 h7b exon 5 F, 5′-Cy5-CAA GGG AAA GCG CCG CTC A-3′; Exon 9 R, 5′-CTC CAT GGC AGG GTT GGC CTC-3′), zebrafish MYH7b (Exon 5 F, 5′-CAT ATA AGG GAA AGC GTC GCT CA-3′; Exon 9 R, 5′-CAG ATG CAA GCT TCC CTG TAG GA-3′), and mouse MYH-β (Exon 6 F, 5′-ACC GGG GCA AGA AGA GGA GC-3′; Exon 9 R, 5′-CTC CAG AGC AGG GTT GGC TTG-3′). The following Northern blotting oligonucleotide probes were used: for miR-208a (5′-ACA AGC TTT TTG CTC GTC TTA T-3′), miR-208b (5′-ACA AAC CTT TTG TTC GTC TTA T-3′), miR-499 (5′-AAA CAT CAC TGC AAG TCT TAA-3′), miR-1 (5′-AAT ACA TAC TTC TTT ACA TTC CA-3′), miR-133 (5′-CAG CTG GTT GAA GGG GAC CAA A-3′), and U6 (5′-CGT TCC AAT TTT AGT ATA TGT GCT GCC GAA GCG A-3′).

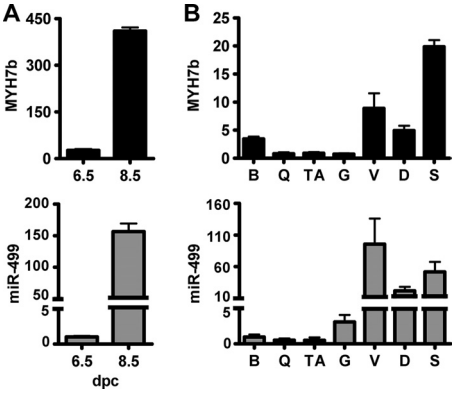

FIG. 1. MYH7b and miR-499 coexpression profile. (A) MYH7b mRNA levels were assayed by real-time PCR performed on cDNA prepared from mouse embryos at 6.5 and 8.5 days postcoitum (dpc) (top). Reactions were normalized to the 18S rRNA. Expression of miR-499, graphed as the fold change in expression from embryonic time point 6.5 dpc to 8.5 dpc (bottom). Quantification of miR-499 was determined using the comparative C_T method from miRNA TaqMan real-time PCR, normalized to snoRNA202. (B) MYH7b mRNA levels were assayed by real-time PCR performed on cDNA prepared from 12-week-old adult mouse brain (B), quadriceps (Q), tibialis anterior (TA), gastrocnemius (G), ventricle (V), diaphragm (D), and soleus (S) (top). Reactions were normalized to the 18S rRNA. miR-499 Northern blot quantification was carried out on the same RNA used for the MYH7b real-time PCR experiments (bottom). U6 snRNA was used as a loading control. Error bars indicate the standard errors of the means calculated from four animals.

RESULTS

The high level of conservation and protein coding capacity across species led us to study the expression patterns of the MYH7b gene and its intronic miRNA, miR-499, located in intron 19. MYH7b and miR-499 expression was measured during fetal development as well as in several adult mouse tissues. Both MYH7b and miR-499 were detected at 8.5 days postcoitum (Fig. 1A) and in adult ventricle, diaphragm, soleus, and, somewhat surprisingly, brain (Fig. 1B). In order to determine the regulatory patterns of MYH7b and miR-499, their responses to thyroid hormone, known to differentially regulate cardiac myosin expression, were tested. MYH7b mimics the well-studied response of MYH-β (15, 29), with an increase in total detected transcripts in PTU-induced hypothyroidism and a decrease in overall expression after PTU treatment and T_3 injections (Fig. 2A, top graph). However, in the presence of the adrenergic agonist phenylephrine, MYH7b is regulated like MYH-α (2), with decreased expression (Fig. 2B, top graph). Overall, as reported for the majority of genes containing intronic miRNAs located in the sense orientation (5), MYH7b and miR-499 showed correlated expression (Fig. 1 and 2, bottom graphs). In agreement with this observation, we did not detect any proximal promoter driving autonomous miR-499 transcription (data not shown).

To gain insight into the role of MYH7b and miR-499 during

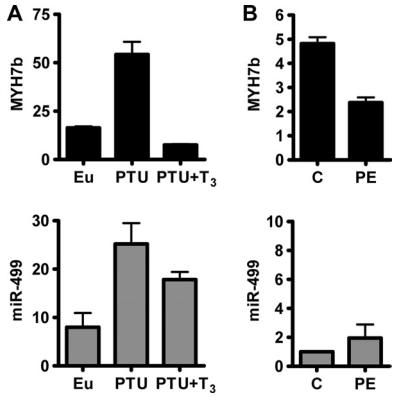

FIG. 2. Regulation of MYH7b and miR-499 expression. (A) Effect of thyroid hormone on the expression of MYH7b and miR-499 in 12-week-old mouse heart. Gene and miRNA expression levels were measured under normal euthyroid (Eu) hormone levels, a PTU-induced hypothyroid condition (PTU), and a hyperthyroid condition due to 2 days of T_3 injection post-PTU ingestion (PTU+T3). Total MYH7b mRNA transcripts in the heart were quantified by real-time PCR and normalized to the 18S rRNA (top). miR-499 Northern blot quantification was carried out on total RNA from the hearts of mice from each thyroid condition, normalized to U6 snRNA (bottom). Error bars indicate the standard errors of the means calculated from four animals. (B) Effect of 48 h of phenylephrine (PE) treatment (20 μM) on the expression of MYH7b and miR-499 in neonatal rat ventricular myocytes. MYH7b expression was measured by quantitative real-time PCR and normalized to 18S rRNA (top). miR-499 expression was quantified by miRNA TaqMan Real-time PCR, graphed as the fold change with PE treatment compared to control levels of miR-499 normalized to snoRNA202 (bottom). Error bars indicate the standard errors of the means calculated from four independent experiments.

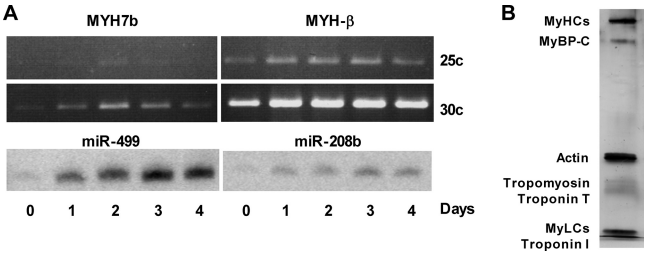

FIG. 3. Comparison of MYH7b and MYH-β gene activity during C2C12 myoblast differentiation. (A) MYH7b and MYH-β mRNA levels were determined by semiquantitative RT-PCR analysis. RNA was isolated from C2C12 cells before differentiation (day 0) through 4 days postdifferentiation (days 1 to 4). PCRs carried out for 25 cycles (25c) and 30 cycles (30c) were resolved on a 2% agarose gel and visualized after ethidium bromide staining (top). Expression levels of the intronic miRNAs, miR-499 derived from MYH7b and miR-208b derived from MYH-β, were determined by Northern blot analysis on the same RNAs used for the RT-PCR analysis (bottom). MYH7b mRNA was translated and found in preparations of myofibril-type proteins. (B) Sarcomeric proteins purified from mouse soleus muscles through differential solubility and centrifugation were separated by SDS-PAGE and detected by silver staining. Purified fractions were then subjected to mass spectrometry analysis. MyHCs, myosin heavy chains; MyBP-C, myosin binding protein C; MyLCs, myosin light chains.

muscle development, we measured their expression in a cell culture model of skeletal muscle differentiation, the mouse C2C12 myoblast cell line. As a control we compared MYH7b to the closely related MYH-β gene, which has been well characterized during muscle development. As shown in Fig. 3A, expression of transcripts of both myosins increased upon differentiation as did expression of their cognate miRNAs. However, the two primary transcripts and their associated miRNAs showed an intriguing discrepancy. While levels of MYH7b mRNA were low compared to the level of MYH-β, miR-499 expression was higher than that of miR-208b. The molecular basis for the relative abundance of the mRNA and miRNA transcripts was elucidated after MYH7b cDNA from both human skeletal muscle and mouse C2C12 cells was sequenced. Exon 7, which encodes the myosin P-loop responsible for binding and hydrolysis of ATP (31), was largely not incorporated into the mature transcript (see below). Exclusion of exon 7 creates a PTC in exon 9 that should activate the nonsense-mediated mRNA decay pathway (NMD), thereby reducing the level of MYH7b mRNA. In addition, this early block should yield a truncated and inactive myosin molecule. However, skipping of exon 7 would not change expression of the intronic miR-499 (located approximately 7.5 kb from exon 7) and/or affect its biological function since pre-miRNA processing occurs in the nucleus, before export and cytoplasmic degradation of the PTC-containing mRNA. Thus, the equal molar ratio between miRNA and host gene mRNA that results from the transcription of a common pre-mRNA is not necessarily reflected by an equal ratio of active products.

We next asked whether MYH7b is a pseudogene, transcribed only to maintain miR-499 expression, or whether production of MYH7b protein could be regulated by alternative splicing. Mass spectrometry was applied to sarcomeric protein-enriched fractions purified from soleus (Fig. 3B) by differential protein solubility (see Materials and Methods). Sequence coverage between 83 to 85% was obtained, with the presence of 125 tryptic peptides unique to MYH7b among myosin heavy chain proteins. The identification of MYH7b protein in a myofibril preparation strongly suggests that it can be incorporated into the contractile apparatus. Moreover, it argues against the hypothesis that MYH7b persists solely to ensure miR-499 expression.

Given that the MYH7b gene can regulate the production of protein via alternative splicing, we decided to examine the *cis* elements of the gene that might contribute to splicing modulation. Analysis of intronic sequences surrounding exon 7 (Fig. 4A) revealed the presence of a conserved U-rich motif located approximately 50 bp downstream of exon 7. U-rich elements appear to be involved in the regulation of a substantial number of alternative cassette exons (3). As expected for alternatively spliced exons (4), we also found that the conservation of exon 7 sequence across different species is greater than that of the corresponding MYH-β exon 7 (Fig. 4B), a characteristic not shared by other MYH7b exons (Fig. 4C).

Since these observations suggest that alternative splicing of exon 7 could be regulated, a systematic analysis was carried out to determine if inclusion of exon 7 occurs in particular cellular environments. As shown in Fig. 5A, several mouse tissues were subjected to quantitative RT-PCR analysis using Cy5 fluorescent primers located in MYH7b exons 5 and 9. The percentage of detected transcripts containing exon 7 ranged from 5 to 6% in brain, diaphragm, and ventricle to 40% in soleus (the PTC

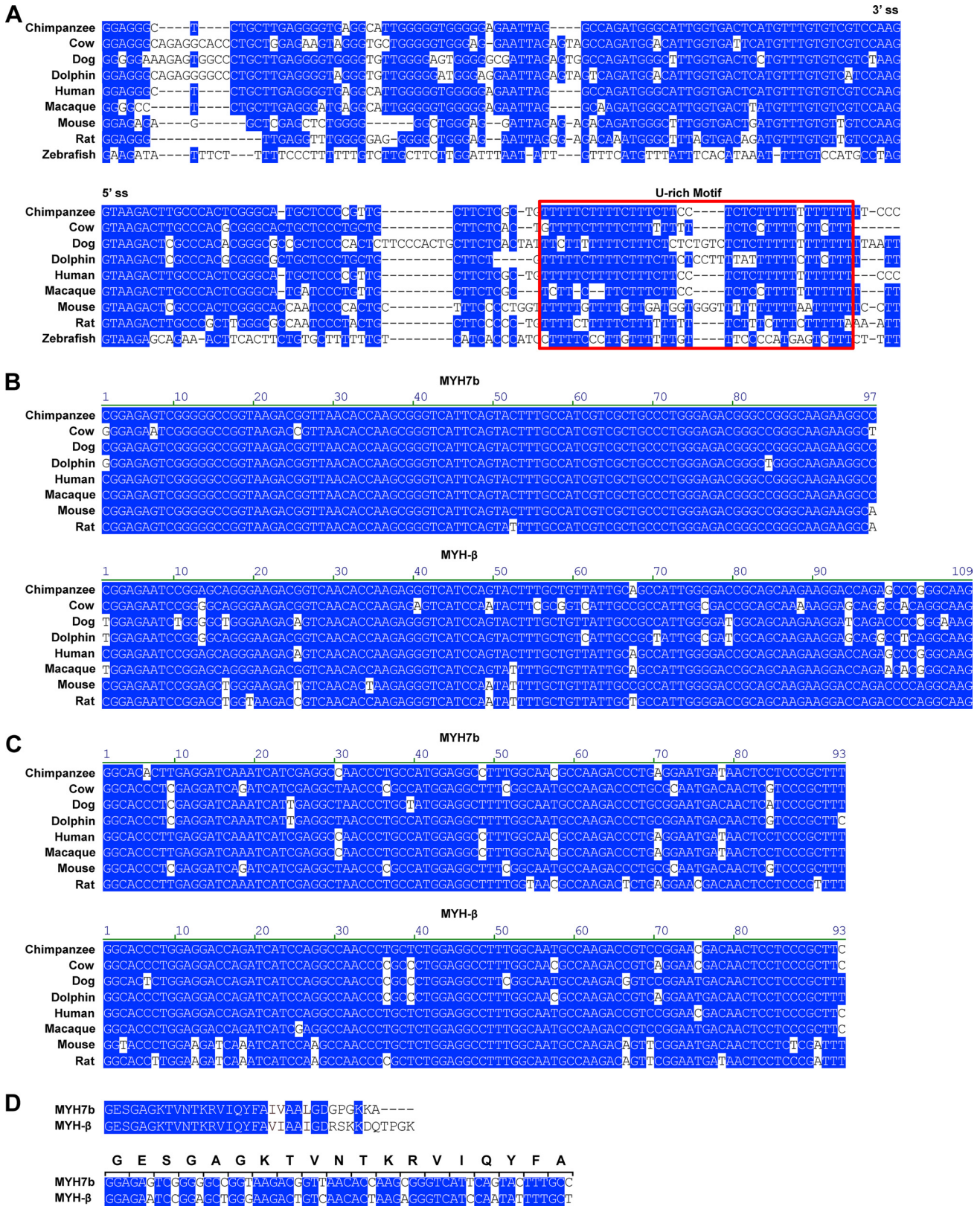

FIG. 4. Sequence analysis of MYH7b exonic and intronic sequences. (A) Comparison of intronic sequences (~100 nucleotides) bordering MYH7b exon 7 across species. The red box indicates the intronic U-rich motif located downstream of MYH7b exon 7. (B) Comparison of exon 7 nucleotide sequence conservation across species for MYH7b (94% identity) and MYH-β (78% identity). (C) Comparison of nucleotide sequence conservation across species for MYH7b exon 9 (79.6% identity) and the corresponding MYH-β exon 8 (78.5% identity). (D) Comparison between MYH7b and MYH-β protein sequences and codon usage in the highly conserved GESGAGK region of exon 7. Protein sequence is conserved to maintain the required GESGAGK motif, but alternate codon usage between the two genes results in differences in nucleotide sequence. In all panels, conserved nucleotides and amino acids are indicated by blue highlighting.

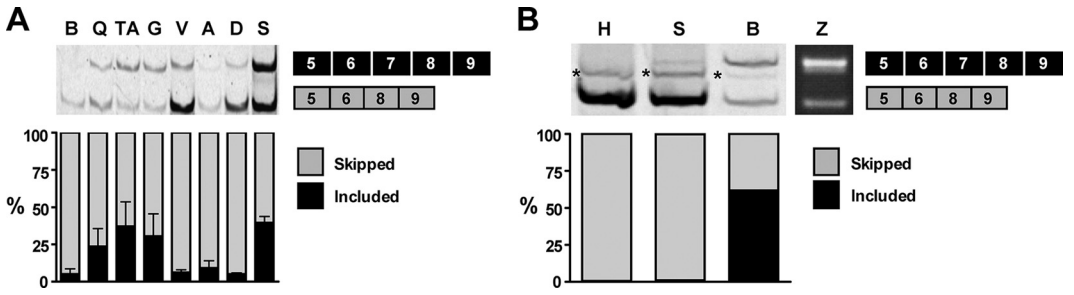

FIG. 5. Alternative splicing of MYH7b exon 7. (A) RT-PCR analysis of RNA isolated from 12-week-old adult mouse brain (B), quadriceps (Q), tibialis anterior (TA), gastrocnemius (G), ventricle (V), atria (A), diaphragm (D), and soleus (S) (top). Reactions carried out with Cy5-labeled primers located in MYH7b exons 5 and 9 were separated by 8% native PAGE and subsequently quantified by phosphorimager analysis. Mobility of the PCR bands corresponding to splicing products that either include or skip exon 7 is indicated. The percentage of exon 7 inclusion or skipping was calculated from tissues of four different mice (bottom). Error bars indicate the standard errors of the means. (B) RT-PCR analysis of human RNA isolated from heart (H), skeletal muscle (S) and brain (B) and RNA isolated from zebrafish (Z) was performed with primers located in MYH7b exons 5 and 9 (top). Reaction mixtures containing Cy5-labeled primers and product quantifications were carried out as described for panel A. Zebrafish products were resolved by 2% agarose gel and visualized after ethidium bromide staining. Each PCR product was purified and sequenced. Asterisks indicate transcripts with skipped exon 7 and activation of a cryptic 5′ splice site downstream of exon 5. Mobility of the PCR bands corresponding to splicing products that either include or skip exon 7 is indicated. The percentage of exon 7 inclusion or skipping in heart, skeletal muscle, and brain, was calculated from several independent experiments (bottom).

created by exon 7 skipping could significantly change the proportion of exon 7-included/skipped mRNAs by triggering NMD). When the survey was extended to human heart and skeletal muscle (Fig. 5B, lanes H and S) we found that inclusion of exon 7 occurred in only 1% of the detected transcripts. In contrast, human brain (from which a full-length expressed sequence tag [EST] was cloned [30]), incorporated exon 7 into a majority of MYH7b transcripts (60%) (Fig. 5B, lane B). Although band intensity suggests that inclusion of exon 7 could produce 2-fold more MYH7b protein in brain, overall gene expression appears to be much higher in muscle. In a small percentage of transcripts, exon 7 skipping also activated a cryptic 5′ splice site located downstream of exon 5 (Fig. 5B, products marked with asterisks). MYH7b exon 7 alternative splicing also takes place in zebrafish (Fig. 5B, lane Z), which also express miR-499 (23). Therefore, synthesis of full-length MYH7b protein could be fine-tuned in a tissue-specific manner by alternative splicing, and MYH7b posttranscriptional regulation is an evolutionarily conserved mechanism.

Since this is the first report of alternative splicing in a mammalian sarcomeric myosin gene, we determined whether alternative splicing of the closely related MYH-β exon 7 occurs. As shown in Fig. 6A (top right panel), alternative splicing does not regulate MYH-β exon 7. Even though this exon shares 100% amino acid sequence identity with MYH7b over the GES GAGK region, at the nucleotide level, changes in the codon usage of MYH7b exon 7 (Fig. 4D) have bypassed the strong coding constraint of the myosin molecule (43). These sequence differences produced different predicted exonic splicing enhancers (ESE) that are recognized by SR proteins (data not shown). Hence, the nucleotide sequence of MYH7b exon 7 could play an important role in regulating alternative splicing.

Expression of MYH-β mRNA in C2C12 cells is approximately 10-fold higher than that of MYH7b, whereas the cor-

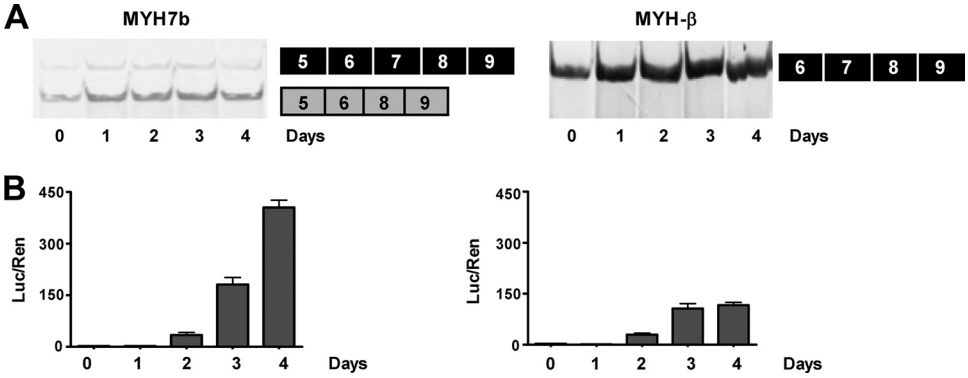

FIG. 6. Comparison of MYH7b and MYH-β exon 7 splicing during C2C12 myoblast differentiation. (A) Splicing of exon 7 of MYH7b and MYH-β was monitored in C2C12 cells before differentiation (day 0) through 4 days postdifferentiation (days 1 to 4) with Cy5-labeled primers, as described in the legend of Fig. 5. Mobility of the PCR bands corresponding to splicing products that either include or skip exon 7 is indicated. The PCR product derived from skipping of MYH-β exon 7 was not detected. A comparison of MYH7b and MYH-β promoter activity during C2C12 myoblast differentiation is shown. (B) The 1-kb promoter regions of MYH7b (left) and MYH-β (right) were cloned in the luciferase reporter plasmid pGL3. Constructs were transfected into C2C12 myoblasts with Lipofectamine 2000, and luciferase activity was measured before differentiation (day 0) through 4 days postdifferentiation (days 1 to 4). Firefly luciferase activity was normalized to *Renilla* luciferase activity. Error bars indicate the standard errors of the means calculated from four independent experiments.

responding miR-208b and miR-499 show the inverse relationship (Fig. 3A). These differences prompted us to analyze the relative activities of the two promoters. After bioinformatics identification of *cis*-regulatory elements of MYH7b, 1 kb of regulatory genomic sequence upstream of the translational start site was cloned into the pGL3 luciferase reporter and transfected into C2C12 cells in parallel with the corresponding region of the MYH-β gene. In agreement with the previous RNA quantification data, this analysis revealed that the activity of both reporter constructs increases during differentiation (Fig. 6B). The observation that the MYH7b promoter is 3-fold more active than that of MYH-β, while its RNA levels are 10-fold lower, supports the hypothesis that the PTC introduced by alternative splicing triggers NMD. To test whether exon 7 skipping activates MYH7b mRNA decay, C2C12 cells were exposed to the protein synthesis inhibitor cycloheximide, previously shown to suppress NMD (7). As hypothesized, the treatment with the drug confirmed the role of NMD in targeting MYH7b transcripts missing exon 7 for degradation. In fact, we observed an increase in the total amount of MYH7b mRNA (Fig. 7A) caused by a selective upregulation of MYH7b mRNA carrying the PTC (Fig. 7C) without changes in the levels of MYH7b containing exon 7 (Fig. 7C and D) or in the levels of MYH-β mRNA, chosen as a control (Fig. 7A). Moreover, the expression levels of miR-499 and miR-208b, used as a control, did not significantly change after treatment (Fig. 7B).

While the production of MYH7b protein may occur in only particular tissues or physiologic states, a broader function of the locus may lie in the activity of miR-499. Among numerous other genes, miR-499 is predicted to target the 3′ UTR of the transcription factor Sox6, which is involved in skeletal muscle development and repression of slow-fiber isoform genes, in particular, MYH-β (17, 18) and potentially MYH7b (13). Recently, miR-499 was shown to target the rat Sox6 3′ UTR (27). To validate Sox6 as a target of miR-499 in mouse, we assayed the ability of miR-499 to repress the activity of a luciferase reporter gene carrying 1 kb of the mouse Sox6 3′ UTR containing four sites complementary to the seed region of miR-499. As shown in Fig. 8A, luciferase activity was reduced approximately 60% in the presence of miR-499 compared to the control transfection. In addition, endogenous levels of Sox6 mRNA were reduced after miR-499 was overexpressed in cardiomyocytes by adenovirus delivery (Fig. 8B). Overexpression of Sox6 in C2C12 cells resulted in (i) repression of a MYH7b 1-kb promoter (Fig. 8C) and (ii) a significant and parallel decrease in both MYH-β and MYH7b and a concomitant activation of MYH-IIb (Fig. 8D). Induction of MYH-IIb suggests that Sox6 is not a general repressor of the sarcomeric myosin heavy chain family. As expected for coregulated intronic miRNAs, the levels of miR-208b and miR-499 mirrored the decrease observed for their host genes (Fig. 8E and F). In addition to Sox6, a number of other predicted miR-499 targets are involved in several aspects of muscle biology: Thrap1 (involvement with thyroid hormone receptor), myostatin (muscle mass and fiber type), Mapk6 (myogenic differentiation), and Sp3 (regulation of MYH-β expression). The experimental validation of these potential targets shows that numerous tissue-specific factors could also be regulated by the miR-499 (Fig. 8G).

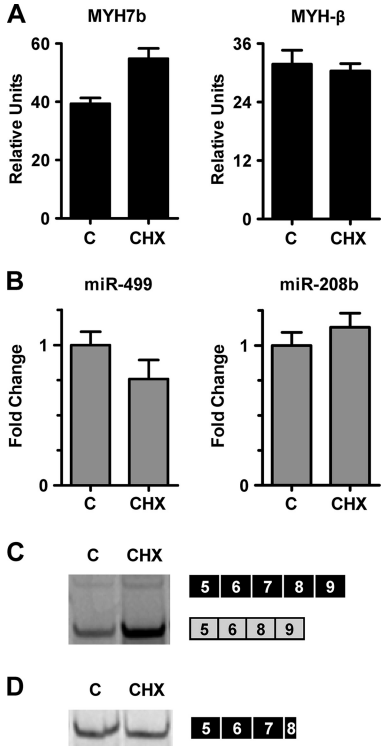

FIG. 7. Cycloheximide treatment of C2C12 cells increases the level of MYH7b mRNA carrying a PTC induced by exon 7 skipping. At 2 days postdifferentiation, C2C12 myotubes were exposed to cycloheximide (100 μg/ml) for 2 h. (A) Total MYH7b and MYH-β mRNA levels were quantified from untreated (C) or cycloheximide-treated (CHX) C2C12 myotubes by real-time PCR as described in the legend to Fig. 1. Error bars indicate the standard errors of the means calculated from three independent samples (MYH7b, $P < 0.05$; MYH-β, $P = 0.69$). (B) miR-499 and miR-208b Northern blot quantifications were carried out on the same RNA used in the experiment shown in panel A. Expression levels of miR-499 and miR-208b were quantified from untreated or cycloheximide-treated C2C12 myotubes as described in the legend of Fig. 1. Cycloheximide treatment did not result in any significant change in either miR-499 or miR-208b expression. Error bars indicate the standard errors of the means calculated from three independent samples. (C) Representative RT-PCR (27 cycles) from RNA isolated from untreated and cycloheximide-treated myotubes was carried out as described in the legend of Fig. 5, with Cy5-labeled primers located in MYH7b exons 5 and 9. Mobility of the PCR bands corresponding to splicing products that either include or skip exon 7 is indicated on the right. (D) Representative RT-PCR (33 cycles) from RNA isolated from untreated and cycloheximide-treated myotubes carried out to detect only transcripts including exon 7. For this experiment the Cy5-labeled forward primer was located in MYH7b exon 5 while the reverse primer was located at the junction of exons 7 and 8. The scheme of the splicing product detected by PCR that includes exon 7 is indicated on the right.

DISCUSSION

The expression of the sarcomeric MYH genes is under the control of complex transcriptional networks (12, 28). Understanding the factors that regulate the expression of the MYH7b gene contributes to the elucidation of its biological function. Our data show that the MYH7b gene shares regulatory patterns with both of the well-studied cardiac MYH genes. However, regulation of MYH7b seems to be less stringently controlled, as evidenced by the expression in brain and the

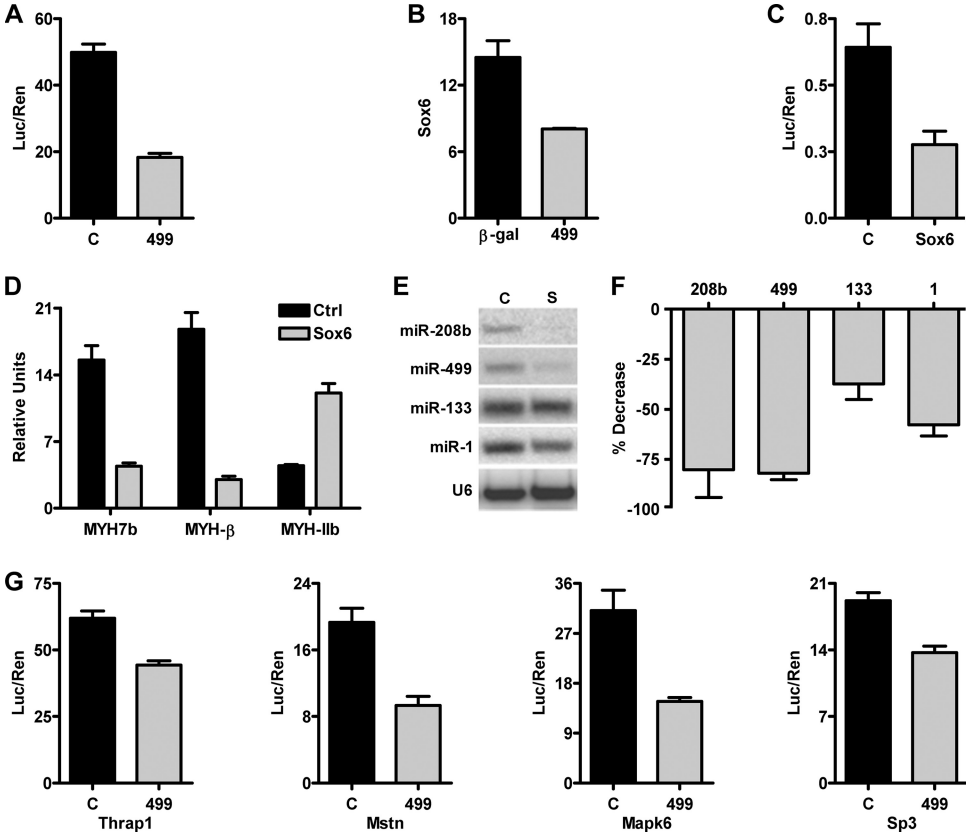

FIG. 8. Analysis of miR-499 predicted targets. (A) COS-7 cells were cotransfected with the pGL-Sox6 reporter, containing 1 kb of the Sox6 3′ UTR fused to the firefly luciferase gene, and the empty vector pcDNA3 used as negative control (C) or an miR-499 overexpression construct (499). Firefly luciferase activity measured 24 h after transfection was normalized to *Renilla* luciferase activity. Reporter activity was significantly decreased after miR-499 overexpression compared to control ($P < 0.01$). Error bars indicate the standard errors of the means calculated from four independent experiments. (B) Neonatal rat cardiomyocytes were infected with a negative-control virus expressing β-galactosidase (β-gal) or a recombinant adenovirus expressing miR-499 (499). Sox6 real-time PCR was performed on total RNA purified 2 days after viral infection. Reactions were normalized to the 18S rRNA. Sox6 mRNA was significantly reduced after miR-499 overexpression ($P < 0.05$); error bars indicate the standard errors of the means calculated from three independent experiments. (C) C2C12 myoblasts were cotransfected with the MYH7b 1-kb promoter and the empty vector pcDNA3 used as negative control (C) or the expression vector pcSox6 (Sox6). MYH7b promoter activity was significantly decreased after Sox6 overexpression ($P < 0.05$); error bars indicate the standard errors of the means calculated from four independent experiments. (D) C2C12 myoblasts were transfected with the empty vector pcDNA3 (Ctrl) or the expression vector pcSox6 (Sox6). Levels of MYH7b, MYH-β, and MYH-IIb mRNA were determined 48 h postdifferentiation by real-time PCR. Each reaction was normalized to the 18S rRNA (relative units). Expression of all three genes significantly changed after Sox6 overexpression ($P < 0.01$); error bars indicate the standard errors of the means calculated from four independent experiments. (E) A representative miRNA Northern blot of total RNA extracted from C2C12 after transfection with the empty vector pcDNA3 (C) or pcSox6 (S) and 48 h of differentiation is shown. U6 snRNA was used as a loading control. (F) Quantification of the Northern blot analysis shown in panel E calculated from four independent experiments. Error bars indicate the standard errors of the means. (G) Validation of additional miR-499 predicted targets. COS-7 cells were cotransfected with a pGL3 reporter containing the 3′ UTR of Thrap1, myostatin (Mstn), Mapk6, and Sp3 with an empty expression plasmid control (C) or miR-499 expression construct (499). Reporter firefly luciferase activity was measured and normalized as above. Activity of all four reporters was significantly reduced after miR-499 overexpression ($P < 0.05$). Error bars indicate the standard errors of the means calculated from at least three independent experiments.

reported detection of miR-499 in the testis, primary human umbilical vein endothelial cells, vascular smooth muscle cells, and human embryonic kidney (HEK 293) and liver carcinoma (HepG2) cell lines (30, 36). The observed changes in MYH7b expression in response to thyroid hormone and PE demonstrate that the gene can respond, as the other cardiac myosins, to different physiological stimuli that play important roles in cardiac function.

The present finding that the MYH7b gene undergoes nonproductive splicing is the first example of a mammalian striated muscle myosin that is regulated posttranscriptionally. Moreover, exon 7 skipping does not generate a new myosin isoform with related or novel physiological function, but it does uncouple the levels of MYH7b transcript from those of the intronic miR-499. In fact, exon 7 exclusion introduces a premature termination codon that (i) prematurely blocks MYH7b translation and (ii) activates MYH7b RNA degradation via the NMD pathway. Since NMD occurs in the cytoplasm, the nuclear production of miR-499 is not affected by the decay process, as confirmed by the cycloheximide experiment (Fig. 7). Importantly, lack of significant accumulation of miR-499 precursor in all cellular settings analyzed rules out posttranscriptional modulation of miR-499 activity by the microRNA processing machinery (data not shown). Thus, by overcoming the

forced coexpression of miR-499 and MYH7b, alternative splicing allows miR-499 expression in tissues where the myosin protein may not be needed. Moreover, it modulates the relative amount of the miRNA and host gene produced. For example, when more miR-499 than myosin protein is required, transcriptional activation of the MYH7b promoter, in concert with exon 7 skipping, increases the expression of miR-499 without a concomitant increase in the levels of MYH7b protein. This model is clearly illustrated in the experiments carried out in C2C12 cells. During cell differentiation we observed more than a 150-fold increase in MYH7b promoter activity (Fig. 6B) that should have been followed by a proportional increase of MYH7b mRNA and miR-499. Instead, the level of the two mRNA populations that include or skip exon 7 (preventing the formation of the PTC or activating mRNA degradation, respectively) rose modestly (Fig. 6A). In contrast, the levels of miR-499 were dramatically upregulated during differentiation and were positively correlated with the promoter activity of MYH7b (Fig. 3), suggesting that the increased amount of primary transcript produced during differentiation skipped exon 7 and was degraded. Importantly, the minor increase in mRNA containing exon 7 (~1.7-fold) suggests that during transcriptional activation the splicing machinery can maintain constant levels of MYH7b by raising the production of more unstable and nonproductive mRNAs which skip exon 7.

In a preliminary bioinformatics analysis carried out on a random sample of 10 genes containing intronic microRNAs, we found that all of them can undergo unproductive splicing and translation (data not shown). Thus, in addition to the presence of dedicated microRNA promoters and cellular modulation of microRNA stability, regulated RNA processing could be another efficient and widespread strategy for uncoupling the expression of biologically active host gene-microRNA products. Interestingly, changes in the expression profile of host genes and intronic microRNAs recently observed in cancer cell lines (34) could be caused by aberrant splicing, often associated with malignant transformation (42). The mechanism of MYH7b alternative splicing may be similar to the *cis*- and *trans*-acting factors that regulate the myosin phosphatase-targeting subunit 1 gene (MYPT1). In this system, the inclusion/exclusion of exon 12 appears to be dictated by an antagonistic competition between the activating T-cell intracellular antigen (TIA) proteins and the repressing polypyrimidine tract-binding proteins (PTBs) for binding of a U-rich intronic region located downstream of the exon 5′ splice site (33). We believe that the synthesis of miR-499 is independent from exon 7 splicing choice. In fact, PCRs performed with a set of primers flanking exon 7 did not detect any obvious delay in the removal of the surrounding introns (data not shown), suggesting that splice site selection is made early during transcription (at an estimated RNA polymerase average elongation rate of 2.4 kb/min, exon 7 becomes available for splicing about 3 min before miR-499 synthesis). Moreover, we determined that miR-499 synthesis can efficiently occur when the microRNA is expressed without the bordering exons (data not shown). Thus, as previously reported for other intronic microRNAs (22), splicing does not appear to play any major regulatory role in miR-499 production.

The high level of protein conservation across several species, the presence of an uninterrupted open reading frame, and the detection of the protein *in vivo* prove that the MYH7b gene is not just a simple molecular container for an intronic miRNA. The low levels of full-length mRNA detected in most tissues do not preclude a potential role for MYH7b in muscle physiology. For example, small changes in the relative expression of the cardiac myosin isoforms MYH-α and MYH-β have significant impact upon cardiac contractility (20).

Intriguingly the human brain has the highest ratio of exon 7 inclusion/exon 7 skipping. Although axonal transport is mainly mediated by several nonconventional single-headed myosins, the double-headed nonmuscle myosin IIB appears to play an important role in dendritic spine morphology as well as in the maintenance of synaptic transmission (32). It is tempting to speculate that MYH7b could be involved in a specific neuronal transport pathway(s). Of interest is the observation that the human gene (but not the mouse gene) encodes an extra 42 amino acids at the beginning of the motor domain (M. L. Bell et al., unpublished data). The mRNA coding for these additional amino acids is expressed only in the brain and theoretically could confer new motor domain properties to the molecule once it is synthesized in the nervous system. Our discovery that in the mouse brain the majority of the MYH7b transcripts do not encode a functional protein suggests the existence of a potential regulatory link between the presence/absence of the 42 extra amino acids and the inclusion/exclusion of exon 7. Thus, as for MYH16 (35), the MYH7b gene could have distinct functions in different species.

We have shown that by targeting the transcription factor Sox6, miR-499 can control its own expression. Transcriptional feedback loops have been previously described for other miRNAs (21, 37, 44, 45), but this is one of the first examples of autoregulation by an intronic miRNA. Sox6 has broad effects in cardiac and bone development, transcriptional repression of slow-fiber-type genes, and regulation of other MYH genes (9, 18, 46). Sox6 also plays a role in central nervous system development (19) and has been detected in the fetal and adult mouse brain (10, 16). Accordingly, miR-499 is expressed in brain (Fig. 1B) where it is coexpressed with MYH7b.

Targeting of Sox6, Thrap1, myostatin, Mapk6, and Sp3 suggests that miR-499 could influence muscle fiber type by fine-tuning the expression of genes that influence muscle development and fiber type specification (11, 14, 26, 38, 39).

In summary, our data show that regulation of the MYH7b gene products is controlled by the coordinate activity of transcription and alternative splicing. Although the functional links between the two cellular machineries are well documented (24), their involvement in modulating the relative expression of an intronic miRNA and its host gene is a novel finding that expands our knowledge of cellular regulatory networks.

ACKNOWLEDGMENTS

This work was supported by NIH grants GM029090 and HL050560 (to L.A.L.).

We thank Daniel Resnicow for his contribution to the identification of MYH7b cDNAs that were missing exon 7, Thomas Armel for his assistance in protein purification, Tom Cheung for PRI algorithm analysis, and Lauren Kiemele of the University of Colorado Cancer Center Proteomics Core for mass spectrometry work. We also thank Tom Blumenthal and Michael Yarus for their critical reading of the manuscript and helpful discussions.

REFERENCES

1. **Allen, D. L., B. C. Harrison, A. Maass, M. L. Bell, W. C. Byrnes, and L. A. Leinwand.** 2001. Cardiac and skeletal muscle adaptations to voluntary wheel running in the mouse. J. Appl. Physiol. **90:**1900–1908.
2. **Antos, C. L., T. A. McKinsey, M. Dreitz, L. M. Hollingsworth, C. L. Zhang, K. Schreiber, H. Rindt, R. J. Gorczynski, and E. N. Olson.** 2003. Dose-dependent blockade to cardiomyocyte hypertrophy by histone deacetylase inhibitors. J. Biol. Chem. **278:**28930–28937.
3. **Aznarez, I., Y. Barash, O. Shai, D. He, J. Zielenski, L. C. Tsui, J. Parkinson, B. J. Frey, J. M. Rommens, and B. J. Blencowe.** 2008. A systematic analysis of intronic sequences downstream of 5′ splice sites reveals a widespread role for U-rich motifs and TIA1/TIAL1 proteins in alternative splicing regulation. Genome Res. **18:**1247–1258.
4. **Baek, D., and P. Green.** 2005. Sequence conservation, relative isoform frequencies, and nonsense-mediated decay in evolutionarily conserved alternative splicing. Proc. Natl. Acad. Sci. U. S. A. **102:**12813–12818.
5. **Baskerville, S., and D. P. Bartel.** 2005. Microarray profiling of microRNAs reveals frequent coexpression with neighboring miRNAs and host genes. RNA **11:**241–247.
6. **Callis, T. E., K. Pandya, H. Y. Seok, R. H. Tang, M. Tatsuguchi, Z. P. Huang, J. F. Chen, Z. Deng, B. Gunn, J. Shumate, M. S. Willis, C. H. Selzman, and D. Z. Wang.** 2009. MicroRNA-208a is a regulator of cardiac hypertrophy and conduction in mice. J. Clin. Invest. **119:**2772–2786.
7. **Carter, M. S., J. Doskow, P. Morris, S. Li, R. P. Nhim, S. Sandstedt, and M. F. Wilkinson.** 1995. A regulatory mechanism that detects premature nonsense codons in T-cell receptor transcripts in vivo is reversed by protein synthesis inhibitors in vitro. J. Biol. Chem. **270:**28995–29003.
8. **Cheung, T. H., K. K. Barthel, Y. L. Kwan, and X. Liu.** 2007. Identifying pattern-defined regulatory islands in mammalian genomes. Proc. Natl. Acad. Sci. U. S. A. **104:**10116–10121.
9. **Cohen-Barak, O., Z. Yi, N. Hagiwara, K. Monzen, I. Komuro, and M. H. Brilliant.** 2003. Sox6 regulation of cardiac myocyte development. Nucleic Acids Res. **31:**5941–5948.
10. **Connor, F., E. Wright, P. Denny, P. Koopman, and A. Ashworth.** 1995. The Sry-related HMG box-containing gene Sox6 is expressed in the adult testis and developing nervous system of the mouse. Nucleic Acids Res. **23:**3365–3372.
11. **Coulombe, P., G. Rodier, S. Pelletier, J. Pellerin, and S. Meloche.** 2003. Rapid turnover of extracellular signal-regulated kinase 3 by the ubiquitin-proteasome pathway defines a novel paradigm of mitogen-activated protein kinase regulation during cellular differentiation. Mol. Cell. Biol. **23:**4542–4558.
12. **Cox, R. D., and M. E. Buckingham.** 1992. Actin and myosin genes are transcriptionally regulated during mouse skeletal muscle development. Dev. Biol. **149:**228–234.
13. **Desjardins, P. R., J. M. Burkman, J. B. Shrager, L. A. Allmond, and H. H. Stedman.** 2002. Evolutionary implications of three novel members of the human sarcomeric myosin heavy chain gene family. Mol. Biol. Evol. **19:**375–393.
14. **Girgenrath, S., K. Song, and L. A. Whittemore.** 2005. Loss of myostatin expression alters fiber-type distribution and expression of myosin heavy chain isoforms in slow- and fast-type skeletal muscle. Muscle Nerve **31:**34–40.
15. **Gupta, M. P.** 2007. Factors controlling cardiac myosin-isoform shift during hypertrophy and heart failure. J. Mol. Cell Cardiol. **43:**388–403.
16. **Hagiwara, N., S. E. Klewer, R. A. Samson, D. T. Erickson, M. F. Lyon, and M. H. Brilliant.** 2000. Sox6 is a candidate gene for p100H myopathy, heart block, and sudden neonatal death. Proc. Natl. Acad. Sci. U. S. A. **97:**4180–4185.
17. **Hagiwara, N., B. Ma, and A. Ly.** 2005. Slow and fast fiber isoform gene expression is systematically altered in skeletal muscle of the Sox6 mutant, p100H. Dev. Dyn. **234:**301–311.
18. **Hagiwara, N., M. Yeh, and A. Liu.** 2007. Sox6 is required for normal fiber type differentiation of fetal skeletal muscle in mice. Dev. Dyn. **236:**2062–2076.
19. **Hamada-Kanazawa, M., K. Ishikawa, D. Ogawa, M. Kanai, Y. Kawai, M. Narahara, and M. Miyake.** 2004. Suppression of Sox6 in P19 cells leads to failure of neuronal differentiation by retinoic acid and induces retinoic acid-dependent apoptosis. FEBS Lett. **577:**60–66.
20. **Herron, T. J., and K. S. McDonald.** 2002. Small amounts of alpha-myosin heavy chain isoform expression significantly increase power output of rat cardiac myocyte fragments. Circ. Res. **90:**1150–1152.
21. **Johnston, R. J., Jr., S. Chang, J. F. Etchberger, C. O. Ortiz, and O. Hobert.** 2005. MicroRNAs acting in a double-negative feedback loop to control a neuronal cell fate decision. Proc. Natl. Acad. Sci. U. S. A. **102:**12449–12454.
22. **Kim, Y. K., and V. N. Kim.** 2007. Processing of intronic microRNAs. EMBO J. **26:**775–783.
23. **Kloosterman, W. P., F. A. Steiner, E. Berezikov, E. de Bruijn, J. van de Belt, M. Verheul, E. Cuppen, and R. H. Plasterk.** 2006. Cloning and expression of new microRNAs from zebrafish. Nucleic Acids Res. **34:**2558–2569.
24. **Kornblihtt, A. R., M. de la Mata, J. P. Fededa, M. J. Munoz, and G. Nogues.** 2004. Multiple links between transcription and splicing. RNA **10:**1489–1498.
25. **Maass, A. H., and M. Buvoli.** 2007. Cardiomyocyte preparation, culture, and gene transfer. Methods Mol. Biol. **366:**321–330.
26. **Manceau, M., J. Gros, K. Savage, V. Thome, A. McPherron, B. Paterson, and C. Marcelle.** 2008. Myostatin promotes the terminal differentiation of embryonic muscle progenitors. Genes Dev. **22:**668–681.
27. **McCarthy, J. J., K. A. Esser, C. A. Peterson, and E. E. Dupont-Versteegden.** 2009. Evidence of MyomiR network regulation of β-myosin heavy chain gene expression during skeletal muscle atrophy. Physiol. Genomics **39:**219–226.
28. **Medford, R. M., H. T. Nguyen, and B. Nadal-Ginard.** 1983. Transcriptional and cell cycle-mediated regulation of myosin heavy chain gene expression during muscle cell differentiation. J. Biol. Chem. **258:**11063–11073.
29. **Morkin, E.** 1993. Regulation of myosin heavy chain genes in the heart. Circulation **87:**1451–1460.
30. **Nagase, T., R. Kikuno, K. Ishikawa, M. Hirosawa, and O. Ohara.** 2000. Prediction of the coding sequences of unidentified human genes. XVII. The complete sequences of 100 new cDNA clones from brain which code for large proteins in vitro. DNA Res. **7:**143–150.
31. **Ruppel, K. M., and J. A. Spudich.** 1996. Structure-function analysis of the motor domain of myosin. Annu. Rev. Cell Dev. Biol. **12:**543–573.
32. **Ryu, J., L. Liu, T. P. Wong, D. C. Wu, A. Burette, R. Weinberg, Y. T. Wang, and M. Sheng.** 2006. A critical role for myosin IIb in dendritic spine morphology and synaptic function. Neuron **49:**175–182.
33. **Shukla, S., F. Del Gatto-Konczak, R. Breathnach, and S. A. Fisher.** 2005. Competition of PTB with TIA proteins for binding to a U-rich cis-element determines tissue-specific splicing of the myosin phosphatase targeting subunit 1. RNA **11:**1725–1736.
34. **Sikand, K., S. D. Slane, and G. C. Shukla.** 2009. Intrinsic expression of host genes and intronic miRNAs in prostate carcinoma cells. Cancer Cell Int. **9:**21.
35. **Stedman, H. H., B. W. Kozyak, A. Nelson, D. M. Thesier, L. T. Su, D. W. Low, C. R. Bridges, J. B. Shrager, N. Minugh-Purvis, and M. A. Mitchell.** 2004. Myosin gene mutation correlates with anatomical changes in the human lineage. Nature **428:**415–418.
36. **Suarez, Y., C. Fernandez-Hernando, J. S. Pober, and W. C. Sessa.** 2007. Dicer dependent microRNAs regulate gene expression and functions in human endothelial cells. Circ. Res. **100:**1164–1173.
37. **Sylvestre, Y., V. De Guire, E. Querido, U. K. Mukhopadhyay, V. Bourdeau, F. Major, G. Ferbeyre, and P. Chartrand.** 2007. An E2F/miR-20a autoregulatory feedback loop. J. Biol. Chem. **282:**2135–2143.
38. **Tsika, G., J. Ji, and R. Tsika.** 2004. Sp3 proteins negatively regulate beta myosin heavy chain gene expression during skeletal muscle inactivity. Mol. Cell. Biol. **24:**10777–10791.
39. **van Loo, P. F., E. A. Mahtab, L. J. Wisse, J. Hou, F. Grosveld, G. Suske, S. Philipsen, and A. C. Gittenberger-de Groot.** 2007. Transcription factor Sp3 knockout mice display serious cardiac malformations. Mol. Cell. Biol. **27:**8571–8582.
40. **van Rooij, E., N. Liu, and E. N. Olson.** 2008. MicroRNAs flex their muscles. Trends Genet. **24:**159–166.
41. **van Rooij, E., L. B. Sutherland, X. Qi, J. A. Richardson, J. Hill, and E. N. Olson.** 2007. Control of stress-dependent cardiac growth and gene expression by a microRNA. Science **316:**575–579.
42. **Venables, J. P.** 2006. Unbalanced alternative splicing and its significance in cancer. Bioessays **28:**378–386.
43. **Weiss, A., S. Schiaffino, and L. A. Leinwand.** 1999. Comparative sequence analysis of the complete human sarcomeric myosin heavy chain family: implications for functional diversity. J. Mol. Biol. **290:**61–75.
44. **Xu, N., T. Papagiannakopoulos, G. Pan, J. A. Thomson, and K. S. Kosik.** 2009. MicroRNA-145 regulates OCT4, SOX2, and KLF4 and represses pluripotency in human embryonic stem cells. Cell **137:**647–658.
45. **Zhao, C., G. Sun, S. Li, and Y. Shi.** 2009. A feedback regulatory loop involving microRNA-9 and nuclear receptor TLX in neural stem cell fate determination. Nat. Struct. Mol. Biol. **16:**365–371.
46. **Zou, L., X. Zou, H. Li, T. Mygind, Y. Zeng, N. Lu, and C. Bunger.** 2006. Molecular mechanism of osteochondroprogenitor fate determination during bone formation. Adv. Exp. Med. Biol. **585:**431–441.